Crack Propagation Characteristics of Coal Samples Utilizing High-Voltage Electrical Pulses

Hongqi Lu,* Yanwei Liu, Baisheng Nie,* Xiujuan Chen, and Xiaokai Xu

ACCESS | Metrics & More | Article Recommendations

ABSTRACT: The technique of high-voltage electrical pulses (HVEP) is a new method to enhance the permeability of coal seams and improve the efficiency of coalbed methane (CBM) exploitation. This paper is aimed at investigating the crack propagation characteristics of samples of different strengths, proposing the improved procedure of HVEP in field application, and proving that the electrohydraulic effect has a wide use in field application of CBM extraction. In this paper, an experimental system utilizing HVEP in water condition is established, coal samples with different strengths are crushed, and the extended processes of cracks are analyzed. According to the research results, the electrohydraulic effect has a good breakage on the coal; the number of main cracks is 2−3 and the length of the main cracks is about 30 cm in the vertical direction of the hard samples; and the formation of cracks is relevant to the discharge voltage, discharge times, and mechanical parameters of the samples. The results of scanning electron microscopy (SEM) demonstrate that the cracks and pore connectivity of the coal samples are improved obviously, and the permeability results show that the permeability of crushed coal samples is 20% greater than that of the raw coal sample. Meanwhile, the generation process of cracks can be divided into four periods: namely, fatigue damage accumulation, slow development, rapid development, and failure; the rapid development stage is the optimal phase in field application. Moreover, the shock wave produced by HVEP via electrohydraulic effect can crush the samples mainly; furthermore, the energy produced by bubble rupture also has a great influence on the formation of cracks. This study can provide a foundation for the HVEP to improve CBM exploitation.
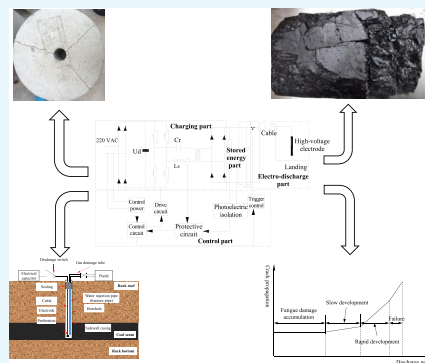
1. INTRODUCTION

Gas drainage is the primary measure to control gas disasters in coal mines.[1] However, more than 70% of the coal seams have low permeability, with a permeability coefficient of $(0.001−0.1) \times 10^{-3}$ mD in China, which greatly affects the efficiency of coal gas extraction, so new methods are needed to improve the permeability of coal seams to promote gas drainage. In the 1950s, Yutkin firstly observed that high-voltage electrical pulses (HVEP) could produce great energy to produce fractures in the laboratory.[2] Since then, the HVEP technology has witnessed a rapid development, and the technology has been widely used in many fields owing to its multiple advantages.[3−5]

In fact, the HVEP can be divided into two categories according to the discharge form: electrohydraulic crushing and electric crushing,[6] of which electrohydraulic crushing is more mature. In electrohydraulic crushing, high-voltage electrodes are discharged in a liquid (usually water), and the high-energy plasma discharge channel is produced at the same time; then, the electric energy will be released via the channel to produce the shock wave and bubbles. For the mechanism of electrohydraulic crushing, Lu et al. firstly observed the bubbles in the process of discharge by high-speed photography and numerical simulation in the laboratory, and inferred that the pressure produced by the bubbles is one-third of the pressure

produced by the shock wave.[7] Kai et al. analyzed the correlation between the pressure of the shock wave, distance of electrodes, and discharge frequency.[8] Andres et al. studied the energy consumption, selective chaining of minerals, and mechanism of electrical disintegration.[9,10]

At present, the technology of solid breaking by plasma is being widely used in many fields, especially in the fields of rock breaking and oil production.[11,12] Zuo separated minerals by virtue of the selective crushing characteristics of HVEP.[13] Bru observed that the mineral particles presented an obvious sorting after breaking the low-grade cassiterite schist.[14] Duan adopted HVEP to recover the metal material from the waste printed circuit board.[15] Patel et al. observed that the plasma pulse technology increased the oil reservoir's natural resonance and reduced adhesion tension, and that the shock wave was also powerful enough to clean perforations near wellbore

damage.[16] Bai et al. studied the effect of rock pore properties on the electric pulse in oil reservoirs.[17] He et al. carried out experiments to study the propagation of the explosion shock wave and the effective range of changes in permeability of the tight sand core samples caused by electrical explosion.[18] Maurel et al. researched the facture characteristic of tight reservoirs and the permeability change under the effect of HVEP, and concluded that HVEP may replace the hydraulic fracturing in oil production.[19]

The use of electrical pulses in enhancing the permeability of coal seam has attracted much attention. Yan et al. conducted experiments to study the effect of HVEP on pore structure and concluded that the pore structure of coal was changed by HVEP, and that the coal presented a burning state in air environment.[20,21] Zhang investigated the influence of electrical fragmentation on the pore structure of coal in air environment.[22] However, the discharging mechanisms of HVEP in air environment and in liquid environment are different: the discharge in liquid is more safe, as it is not easy to damage the electrodes. Electrohydraulic crushing has the advantage of repeating the discharge. The application of electrohydraulic crushing in CBM extraction has started in the recent years. Li et al. found that the pore structure of coal can be changed by the shock wave produced by HVEP, and proposed the scientific problems to be solved of using HVEP in enhancing the permeability of coal seams.[23,24] Ma suggested that the electrohydraulic crushing could enable the coal body to produce open-type and sliding-type cracks mainly.[25] In field application, Zhang provided a successful demonstration in a coal mine, and the applied results showed that the permeability of the coal seam was enhanced obviously, and that it saves most of the hole engineering work.[26,27] Wu, Guo, and Zhang showed that the electrohydraulic effect could remove blockages in the cracks; however, the engineering order should be improved, and the technology also has its limits, such as the characteristics of the coal seam reservoir.[28−30] In previous work, the coal hardness, not the metamorphic grade, has been shown to have a great effect on the electrohydraulic crushing.[31] Nevertheless, the influence of the varying hardness of different coal samples on the electrohydraulic effect has been rarely reported, and the operation sequences of the technology should be optimized. Hence, it is novel and meaningful to prepare different samples and conduct research on the crack propagation features under the electrohydraulic effect.

In this study, a HVEP experimental system was built, and different samples were tested to investigate the distributed and extended features after crushing coal by the HVEP technology. Meanwhile, the mechanism and different applications of HVEP were also analyzed. The study results will provide new ideas for the application of HVEP to improve CBM exploitation.

2. RESULTS AND DISCUSSION

2.1. Distribution Features of Cracks in Similar Samples.
After discharging many times by HVEP, all similar samples were fractured. The experimental parameters, including the electric field strength and the discharge times, are presented in Table 1, and the distribution features of the cracks after breakdown are shown in Figure 1. In these experiments, the 1# sample was fractured after acting 13 times, the 2# sample was fractured after acting 11 times, the 3# sample was fractured after acting 7 times, and the 4# sample was fractured after acting 2 times. The experimental results show that the number of main cracks is 2−3, and the

Table 1. Experimental Parameters of Similar Samples

number of similar samples	U (kV)	d (cm)	E (kV·cm)	capacitance (μF)	discharge times
1#	13	0.8	16.25	10	13
2#	13	0.8	16.25	10	11
3#	11	0.8	13.75	10	7
4#	9	0.4	22.5	200	2

distribution of the cracks is relatively symmetrical. The lengths of the main cracks in all samples are presented in Table 2. Figure 1 and Table 1 show that when the discharge times decrease with the electric field strength and the capacitance increases, the formation of cracks is relevant to the discharge voltage, the crushing times, and the mechanical parameters of the samples. With the strength of the samples increasing, the lengths and number of cracks also are increasing. Figure 1b also shows that when the shock wave meets the structural defects of the sample, the cracks will swerve along the defects and make the crack network more complex.

Figure 1 illustrates that all samples fracture after acting many times, and shows that the HVEP has an obvious effect on the crushing of the samples. After breaking by the electrohydraulic effect, the samples show some cracks that are decussate. In the acting process of HVEP, the shock wave can crush the samples to make main cracks extend in water condition; cracks are also produced along the main cracks, and thus, the fracture network forms to encourage the extraction of CBM.

2.2. Distribution Features of Cracks in the Coal Samples.
The experimental parameters of the coal samples are presented in Table 3, and comparison of the cracks before and after discharging is shown in Figure 2. In the experiments, the conversion efficiency of the discharge energy was about 30%,[34,35] so the discharge energy was 181.5 J per unit of time. Every coal sample was crushed 5 times, with the interval between every discharge being 15 s.

As shown in Figure 2, all coal samples are crushed after discharging by HVEP, and the crack connectivity increases evidently. For 1# coal sample, after the first discharge, the face of the coal sample shows a few cracks without damage. After the second discharge, the length of the original crack is extended, new cracks appear, and some small coal particles are produced; however, the coal sample still is complete. After the third discharge, the length and width of the cracks extend quickly, and large coal particles of the right part of the coal sample drop. After the fifth discharge, some new macro-fractures appear, and the coal samples crush. The same is true for the other samples.

The scanning electron microscope (SEM) was used to analyze the surface changes of the coal samples. In order to ensure the reliability of the results, the coal particles of 3# coal sample before and after breaking used for SEM are collected at the same position that is directly below the positive electrode, and the SEM results are shown in Figure 3. Because the coal samples are hard relatively, few cracks and pores existed in the original coal sample, and the connectivity of the pores and cracks is poor. However, the pores and cracks increase, and the connectivity is improved obviously after breaking. In Figure 3, the shock wave produced by HVEP can be seen to ameliorate the network of pores and cracks of the coal samples, so the migration pathways of methane in the coal body are smooth after crushing, and thus the permeability of coal can be improved.
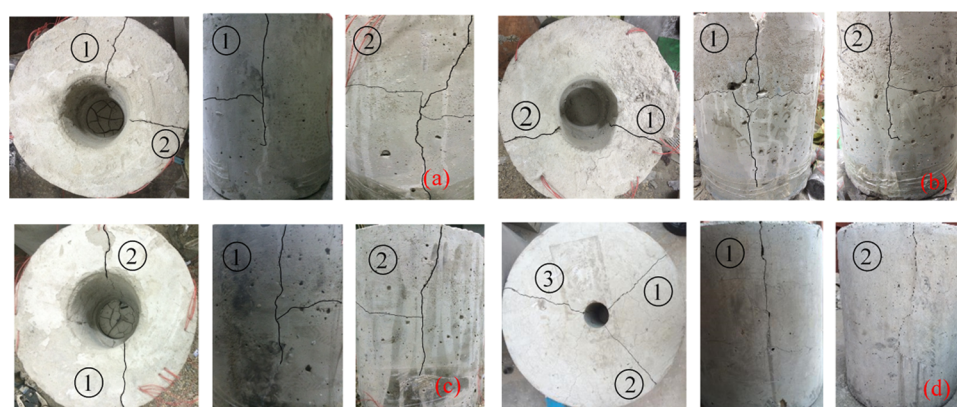
Figure 1. Crack distribution features of similar samples: 1# similar sample (a), 2# similar sample (b), 3# similar sample (c), and 4# similar sample (d).

Table 2. Length of Main Cracks in All Samples

number of the sample	1#	2#	3#	4#
				①: 28 cm
	①: 25 cm	①: 31 cm	①: 25 cm	
the length of main cracks				②: 27 cm
	②: 29 cm	②: 25 cm	②: 26 cm	
				③: 30 cm

Table 3. Experimental Parameters of the Coal Samples

number of sample	U (kV)	d (cm)	E (kV·cm)	capacitance (μF)	discharge times
1#	11	0.5	22	10	5
2#					
3#					

The permeability of the coal sample after electrohydraulic crushing was tested, and the result is illustrated in Figure 4. In the test, the gas pressure is 0.7 MPa and the confining pressure is 1.2 MPa. The results reveal that the permeability of the crushed coal sample is greater than that of the raw coal sample, which is increased by about 20%, and suggest that the electrohydraulic effect can break the coal sample obviously to produce more cracks and pores, and the permeability of coal can also be enhanced. Moreover, to ensure the integrity of the coal sample to drill the cylindrical sample for the permeability test, the measured permeability growth rate may be kept lower than that in field application.

2.3. Extension Features of Cracks. The experimental results of similar samples and coal samples show that the HVEP can produce large amounts of new cracks and pores for methane migration, so the methane can flow quickly and fluently. For similar samples, the number of main cracks is 2–3, and the main cracks appear from the top of samples, then extend to the bottom of the samples. The distribution features of main cracks and branch cracks are presented in Figure 5.

For similar samples, the extension feature of the main cracks produced after crushing multiple times is the same, taking 3# sample as an example in this paper. The extension process of the main crack on 3# sample is presented in Figure 6, and the main crack on the top of the sample after acting 8 times is shown in Figure 8c. In Figure 6, there is no crack in the sample after discharging 5 times (Figure 6a,b); the microcrack is produced at the top of sample, which is near the borehole after

discharging 6 times (Figure 6c). The crack extends from the top to the bottom of the sample after discharging 8 times (Figure 6d), and it extends to the bottom of the sample until the sample is crushed after discharging 9 times (Figure 6e,f), with the length and width of the main crack increasing. After discharging 12 times, 3# similar sample is broken into two pieces.

In order to analyze the crack changes of the coal samples, the coal particles at the same position of 3# coal sample after each discharge are collected. Then, the cracks number of the coal particles is observed after enlarging 20-fold, with the observation scope about 1×1 cm^2. The relationship between the discharge times and crack changes is shown in Figure 7a, and the discharge channel in the coal sample is shown in Figure 7b. In the experiment of crushing the coal samples, after discharging 2 times, the crack density is not increased significantly. After discharging 4 times, the crack density of the coal samples increases quickly and the macrofractures appear. After discharging 5 times, a large amount of macrofactures and macropores appear, and the particles of the coal samples collapse. With the discharge times increasing, the fracture degree, crack propagation, and crack density of the coal samples increase faster and faster. From the discharge channel of the coal sample, the technique of HVEP cannot produce a high temperature to burn the coal body around the channel and affect the coal body via electrohydraulic effect, which shows that the HVEP technology is safe in field application.

Based on the comprehensive analysis of the experimental results of similar samples and coal samples, the propagation process of the cracks produced by HVEP is shown in Figure 8. The results suggest that the extension process of cracks can be divided into four stages: namely, fatigue damage accumulation stage, slow development stage, rapid development stage, and failure stage. In the fatigue damage accumulation stage, there are no or few microcracks in the samples after discharging sometimes, and the pulsed stress is accumulated in the crack tips via water. In the slow development stage, the microcrack is produced; however, the growth rate is small, and few microcracks are produced. In the rapid development stage, microcracks and micropores develop rapidly, the branch cracks are also produced, and at the same time, the length and width of the main cracks increase quickly. In the failure stage, macro-cracks develop quickly, and the particles collapse until the sample is broken. From the experiments, it can be seen that the
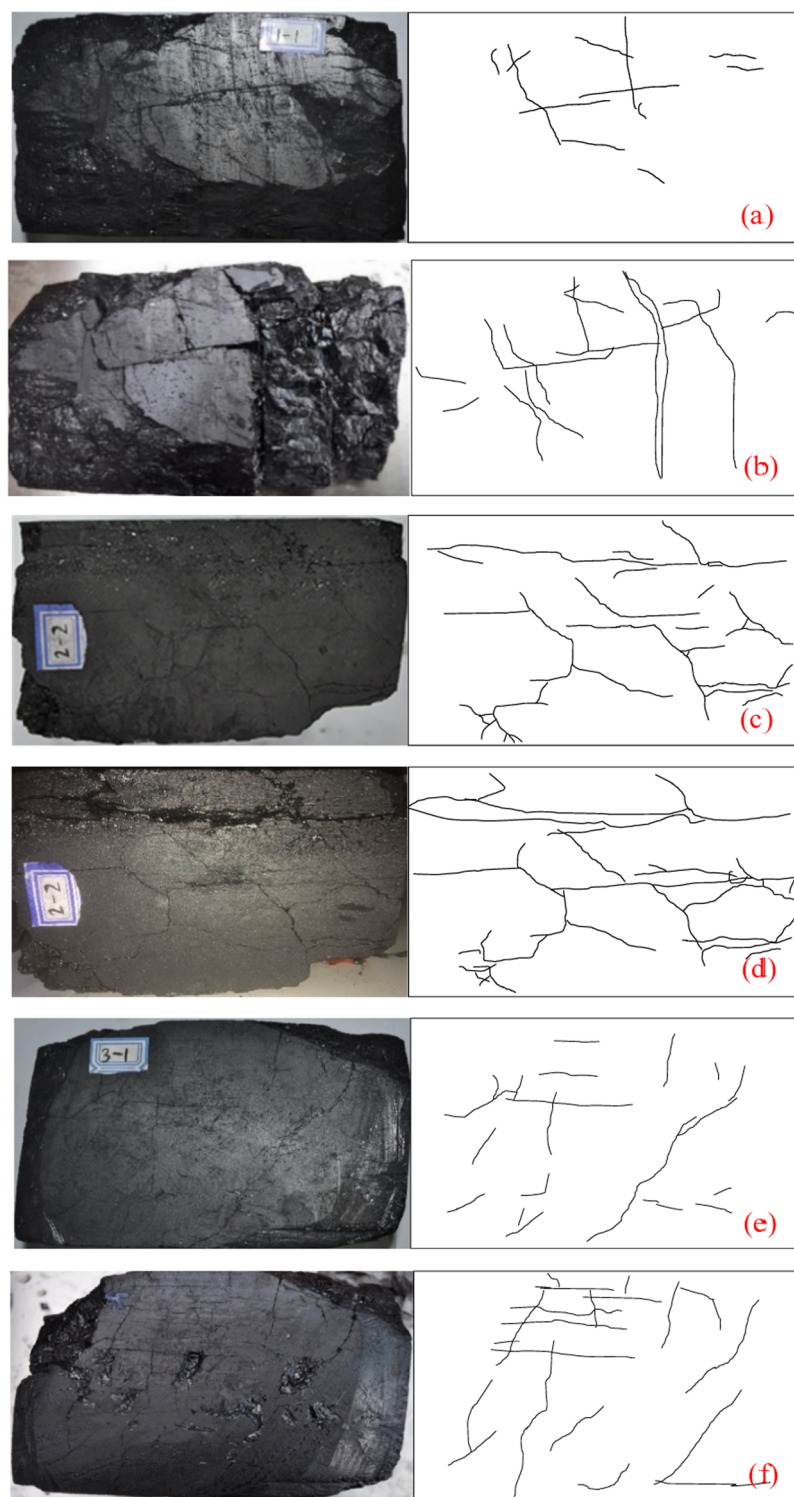
Figure 2. Crack distribution and sketches of the original and crushed coal samples: 1# original coal sample (a), 1# crushed coal sample (b), 2# original coal sample (c), 2# crushed coal sample (d), 3# original coal sample (e), and 3# crushed coal sample (f).

third stage is the optimal period for enhancing the permeability of the coal seams, namely the rapid development stage. In the third period, the crack network is produced, the permeability of coal seam is enhanced without pulverized coal blockage, and it can provide a smooth migration channel for methane. However, the accurate crushing times have to be determined by the field application.

2.4. Crushing Mechanism of HVEP. The mechanical energy and heat energy are transmuted by electric energy, and the process can be divided into the following steps:[2] (1) when the charge energy meets the breakdown voltage, the liquid in the discharge channel is broken down, and then the electrodes start discharge. (2) After the channel is broken down, the liquid around the channel will be gasified and expanded instantly, so the shock wave will be produced. (3) In the end of
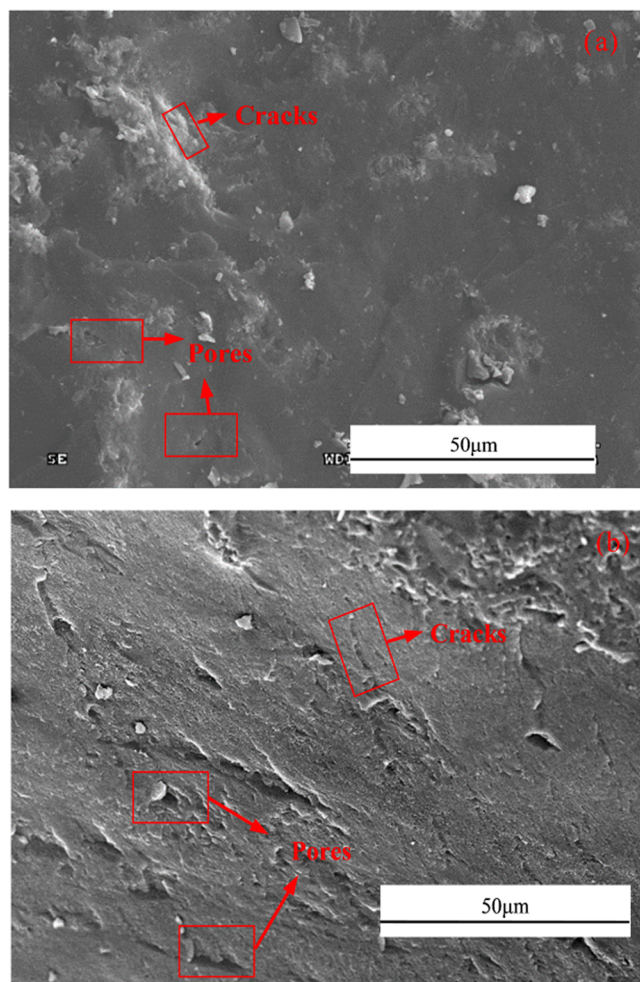
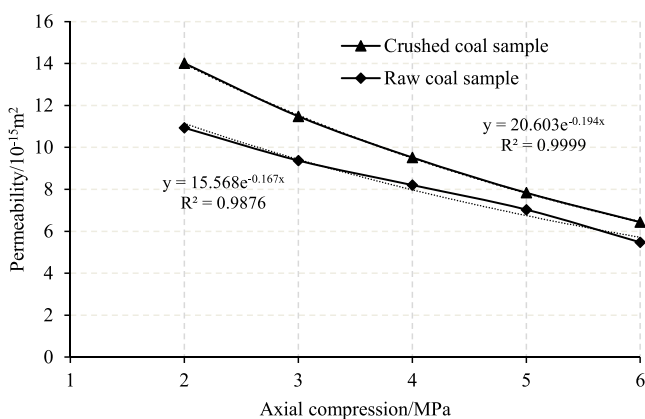**Figure 3.** Surface changes of the coal samples: origin coal sample (a) and crushed coal sample (b).

Figure 4. Permeability comparison of the crushed coal sample and the raw coal sample.

Figure 5. Main and branch cracks on similar samples: main cracks (a) and branch cracks (b).

In fact, coal is not only of a heterogeneous matter, but also a natural organic rock with complex pores and fractures, and this aspect makes coal non-uniform in mechanical properties.[36,37] In the functional process of HVEP, the shock wave can produce a tangential stress to compress the coal body. Assuming the pressure of the shock wave is p_s, it is given by

$$p_s = p_m e^{-\gamma r/u_s} = \beta \sqrt{\frac{\rho_0 W}{\tau T}} e^{-\gamma r/u_s} \qquad (1)$$

where γ is the attenuation coefficient of the shock wave, r is the distance between the tested point and the discharge channel, and u_s is the propagation velocity of shock wave.

When the liquid around the discharge channel is gasified to be gas with high temperature and high pressure, the temperature difference between the gas and the liquid is rendered big enough to produce bubbles, and then the bubbles will diffuse outward from the point of discharge. There are lots of cracks and pores in the coal body, so the migration channels of bubbles are unconnected. When the bubbles meet the coal, the pressure balance inside and outside the bubbles will be broken, the bubbles will appear distorted until they break off, and the microjet may be produced in the process of the bubble break, so the pressure will be produced to fracture the coal when the bubbles are broken.[38,39] Assuming the pulsating pressure of a single bubble is p_b, it may be calculated as[40]

$$p_b = \rho_0 (R_b^2 \overset{g}{R_b} + 2R_b^2 \overset{g}{R_b})/r - R_b^2 R_b^4/2r^4 + p_0 \qquad (2)$$

where ρ_0 is the density of the liquid, R_b is the radius of the bubbles, $\overset{g}{R_b}$ is the derivative of the bubble radius to time, and p_0 is the hydrostatic pressure.

So, assuming the total pressure of the crack is p_t,

$$
\begin{aligned}
p_t &= p_s + p_b + p_0 \\
&= \beta \sqrt{\frac{\rho_0 W}{\tau T}} e^{-\gamma r/u_s} + \rho_0 (R_b^2 \overset{g}{R_b} + 2R_b^2 \overset{g}{R_b})/r - R_b^2 R_b^4/2r^4 \\
&\quad + 2p_0
\end{aligned}
\qquad (3)
$$

Coal is a complex medium, and its cracks are type I and type II mainly, namely the opening-mode edge cracks and the sliding-mode edge cracks. Assuming the tip stress of cracks is σ_θ,

$$\sigma_\theta = \frac{1}{2(2\pi r)^{1/2}} \cos\frac{\theta}{2} [K_I(1 + \cos\theta) - 3K_{II}\sin\theta] \qquad (4)$$

where θ is the angle between the new crack and original crack, K_I is the intensity factor of the opening-mode edge cracks, and K_{II} is the intensity factor of the sliding-mode edge cracks.

the discharge, the bubbles will be produced because of the electric field, they will break to produce the mechanical energy, and the energy spreads outward in a spherical shape. (4) All energy produced by the shock wave and the bubbles decrease in the coal body exponentially. If the energy is greater than the strength of the coal body, the coal will fracture; otherwise the process will stop.
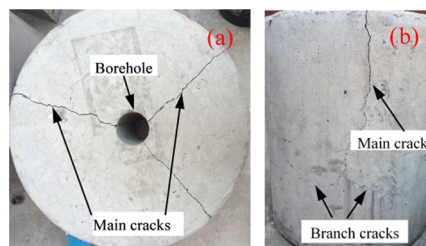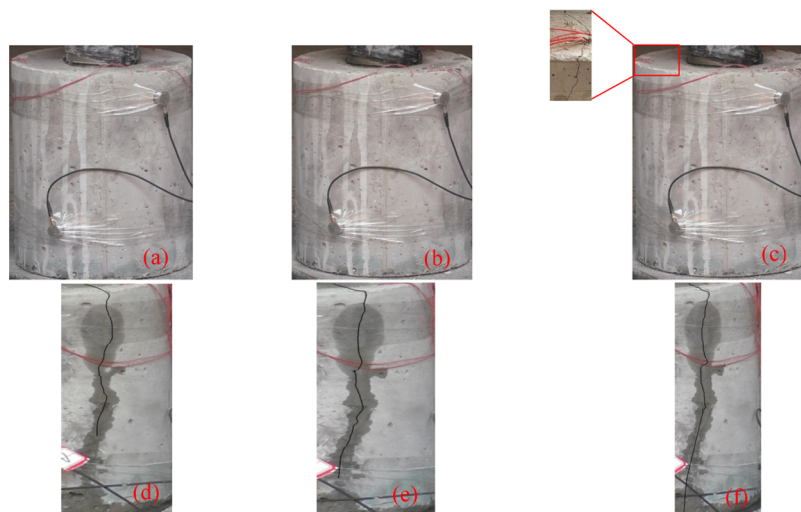
Figure 6. Extension process of the main cracks of 3# similar sample: 1 time discharge (a), 5 times discharge (b), 6 times discharge (c), 8 times discharge (d), 10 times discharge (e), and 11 times discharge (f).
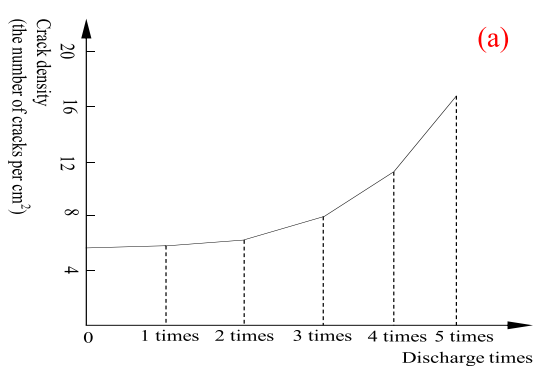

Figure 7. Crack propagation process: relationship between the discharge times and crack density (a), and the discharge channel in the coal body (b).
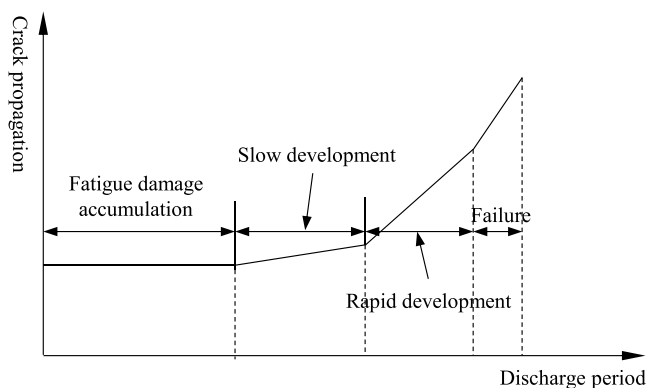

Figure 8. Process of crack propagation.

When the pressure p_t is greater than the tip stress of the coal body σ_θ, new cracks will be produced and thus the coal body will be broken. At the same time, the strength of the coal body will be decreased under the multiple actions of the shock wave in a short period, so the pressure will be concentrated under the impact of the shock wave in water condition to produce more cracks. At the same time, the shock wave can make vibrations at the contact area of coal and water because of the different propagation velocities in the coal and water, so the solid particles in the cracks in the coal body can be eliminated.

These aspects can encourage the coal seam to produce more cracks. In the functional process of HVEP, some heat energy may be produced because of the energy transformation, leading to the adsorption of methane and changing it to the flow gas in the coal seam.

Generally, the fracture mechanism of HVEP includes the following aspects: First, the shock wave produced by HVEP creates cracks in the coal seam. Second, the pressure released by the bubbles produced by HVEP promotes the formation of new cracks and pores. Third, the stemming-in fractures can be eliminated via vibration and produce some heat in the discharge process of HVEP, and this helps the gas flow in the coal seam.

2.5. Application in CBM Exploitation of the HVEP Technology. The output process of CBM includes three phases, namely gas desorption, diffusion, and seepage. Gas desorption and diffusion occur in the micropore, and gas seepage often occurs in the mesopore, macropore, and cracks, so the crack network in the coal seam has an obvious effect on the CBM output. As shown in Figures 5−7, the huge energy produced by HVEP can break down coal samples, and the new crack network is produced, which is conducive for gas seepage to increase the CBM production.

The HVEP technology has been used in shale gas exploitation and oil production; however, CBM exploitation
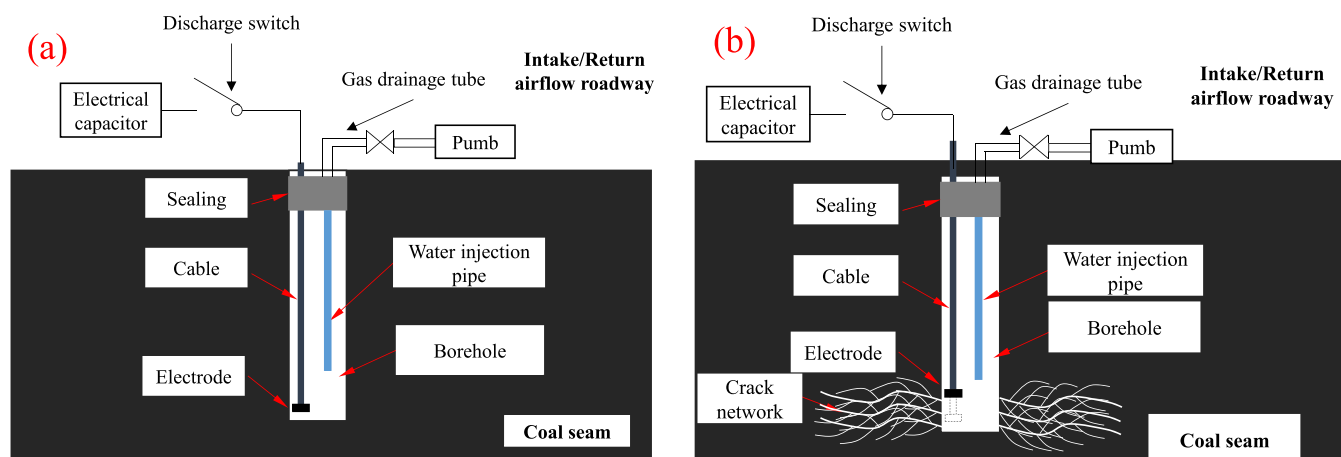
Figure 9. Application of HVEP in the coal face: before crushing (a) and after fracturing a segment (b).
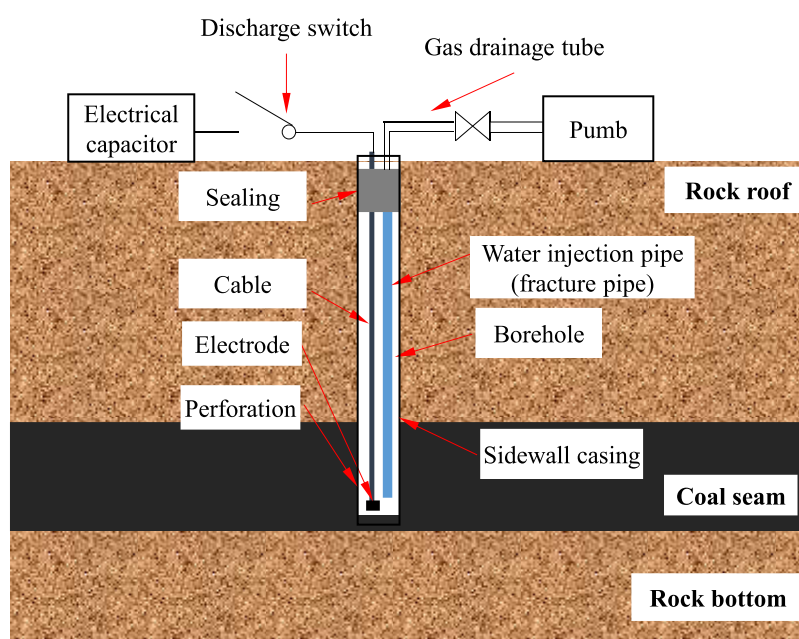

Figure 10. Application of HVEP in a surface CBM well.

is different from oil exploitation. At present, methane drainage underground accounts for about 75% in total, and the utilization rate of methane extracted underground is about 56% in China.[41] It is obvious that enhancement of the permeability of coal seams by the HVEP technology underground is a key method to improve the CBM exploitation.

When the HVEP technology is used to increase the permeability of coal seam underground, the details of the technology are as follows: (1) A drainage borehole is drilled from a roadway to the coal seam. (2) The electrode is placed in the borehole (the electrodes are connected to the HVEP system), and some water is injected via a pipe into the borehole to provide the discharging liquid environment. (3) The borehole is sealed by special material, and then charge provided to the capacitor. (4) The switch is opened to crush the coal seam segmentally until the amount of crushing time to achieve the calculated amount according to the field situation. (5) The above steps are repeated until the whole borehole is crushed in a vertical direction. (6) The electrodes are taken out

from the borehole, and then the borehole is connected to the gas drainage system.

During the electrical breakdown process, the equipment can be placed in the intake airflow or return airflow roadway. In order to enhance the permeability of the coal seam, the guide hole can be completed near the drainage borehole. The application procedure of HVEP used underground is shown in Figure 9.

In light of the successful application of HVEP in oil production, the new method of enhancing the permeability by utilizing HVEP based on compound fracturing is in use.[42,43] Owing to the difference of the drainage holes and the coalbed methane wells, the applied process should be improved.

When the HVEP technology is used on the ground, the system of HVEP in a surface CBM well is shown in Figure 10. The HVEP can crush the coal seam without damaging the sidewall casing in the CBM well.[44] So the applied process based on HVEP is as follows: (1) A CBM well is completed from the ground in the non-mining area, and then the sidewall casing with perforation is placed into the well to protect the
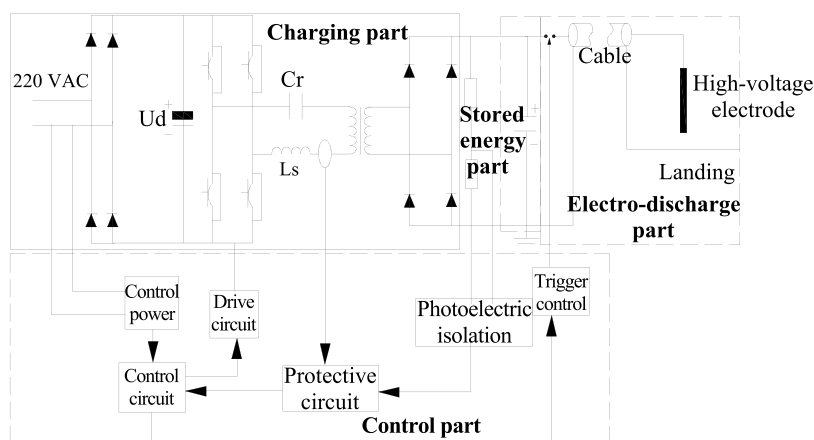
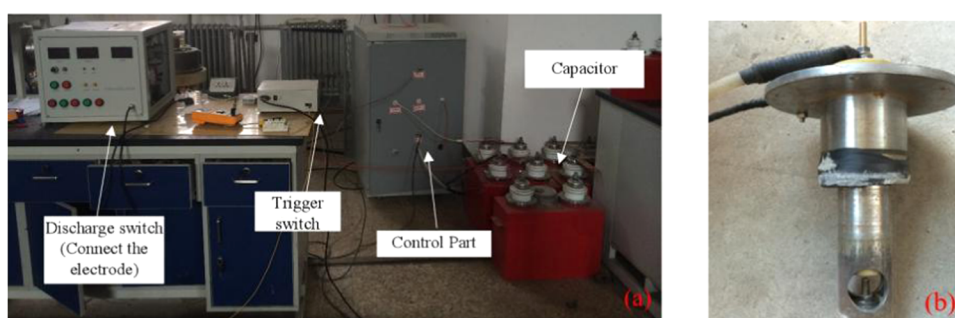**Figure 11.** Schematic diagram of the HVEP system.

Figure 12. Experimental system: the physical diagram (a) and the electrode (b).

well. (2) Some water with a certain pressure and proppant along the perforation is injected into the well to fracture the coal seam, then the electrodes are put into the well, and the well is sealed above the electrodes by some material. (3) The capacitor is charged until the stored energy reaches the preset value, then the discharge switch is turned on, and the energy is released into the perforation to break down the coal seam. (4) The discharge step is repeated to achieve a higher permeability according to the field situation. (5) After the discharge step, the drainage pump is applied to expel the water and the electrodes are taken out from the well, then the well starts to extract. Owing to the less quantities and low cost, HVEP also can be used for secondary fracturing.

In field application of HVEP, regardless of the application method, based on the experimental results and the mechanism of HVEP, the basis of the technology is discharging on one site of the borehole or well repeatedly, crushing many sites consecutively, ensuring the crush is done in a segmented operation, and discharging along the whole hole to enhance the permeability of the coal seams. The drainage borehole layout should be optimized according to the coal seam.

3. CONCLUSIONS

The crack propagation characteristics of different-strength samples and the permeability changes of coal samples are investigated utilizing a self-designed electrohydraulic crushing experimental system. The results indicate that the electro-hydraulic effect has a great influence on the formation of cracks. According to the breakdown results of the high-strength samples, the electrohydraulic effect can produce cracks of large scale that are more than 30 cm; the symmetrical crack network is produced when the electrode discharge occurs in a borehole;

and the discharge times are related to the electric field, the capacitor, and the mechanical parameters of the samples. The results of coal samples show that the connectivity of cracks and pores in the coal body after breaking is better, the permeability is increased by more than 20%, and the coal body around the discharge channel is not burning, which shows that the HVEP is safe and practical for field application. By integrating the crack propagation of different samples, the process of cracks can be divided into four stages, and the third phase, namely rapid development stage, is the optimal condition for field application. Besides the shock wave, the energy produced by bubbles also has an obvious effect on the formation. Based on the feasibility of the electrohydraulic effect on the samples, the improved method for permeability enhancement is proposed.

4. EXPERIMENTS

4.1. Experimental System. The schematic diagram of the experimental system is illustrated in Figure 11; the system consists of four subsystems, namely charge system, energy-stored system, control system, and electro-discharge system. The functional processes of HVEP are as follows: (1) the regular alternating electric current (220 V/50 Hz) is transformed into a high-voltage direct current (about a few 10 s of kV) via the charge system; (2) the high-voltage direct current is used to charge the electrical capacitor; and (3) the discharge switch is opened to supply electrical power to the electrode when the discharge level increases to meet the breakdown field strength, and then the electrode crushes the samples. The physical diagram of the experimental system and the electrodes is shown in Figure 12.

4.2. Similar Samples Preparation. In order to analyze the crack propagation of different samples, two kinds of

Table 4. Proportions of Similar Samples

number	size (mm)	cement (%)	sand (%)	gypsum (%)	mica powder (%)	parameters of boreholes (mm) depth	diameter	compressive strength, p (MPa)
1#	$\varphi 300 \times 300$	27.7	66.9	4.9	0.5	150	100	4.3
2#	$\varphi 300 \times 300$	34.5	60.3	4.3	0.9			6.5
3#	$\varphi 300 \times 300$	25.3	70.5	3.6	0.6			12.6
4#	$\Phi 500 \times 500$	33	67			250	60	29.7

Table 5. Sizes and Proximate Parameters of the Coal Samples[a]

number	sizes (mm)	proximate analysis (%) M_{ad}	A_{ad}	V_{daf}	FC_d	consistent coefficient, f	compressive strength, p (MPa)
1#	$150 \times 9\ 0 \times 70$	1.29	11.78	9.23	77.7	0.45	4.1
2#	$140 \times 125 \times 85$						
3#	$150 \times 100 \times 90$						

[a]Note: M_{ad} and A_{ad} represent the moisture content and ash content on air-dried basis, V_{daf} is the volatile matter content on dry-ash-free basis, and the FC_d is the fixed carbon on air-dried basis.

samples were made, namely similar samples and coal samples. Because of the unique characteristics of coal samples, it is difficult to collect large coal samples in coal mines. Hence, in order to analyze the crack propagation characteristics of samples of different strengths, some similar samples were made for the experiment.

According to the results of previous studies,[32,33] some materials were chosen to make similar samples, which were used to simulate coal samples of high strength. The similar samples were made of cement, sand, gypsum, and mica powder. Two different sizes of cylinder samples were made for the experiments: $\varphi 300$ mm $\times$ 300 mm and $\varphi 500$ mm $\times$ 500 mm. The mass ratios, sizes, and compressive strength of the samples were determined as shown in Table 4. In order to place the electrode, the boreholes were preset in the middle of the samples; the related diameters of the boreholes are shown in Table 1. After maintaining for 28 days, these samples could be used for experiments.

4.3. Coal Sample Preparation. The coal samples were obtained from Lu'an coalfield, which is located in the southeast of Shanxi province; these samples were collected from the fresh working face and then sent to the laboratory for the experiments. The sizes and proximate analysis of the coal samples are presented in Table 5. Because the coal samples were soft relatively, and due to the limits of the fixed position in the box which is made to place coal samples (as illustrated in 4.4), it was difficult to make the sizes uniform.

According to Table 5, the mechanical parameters of similar samples are similar to those of raw coal samples, and the similarity ratio is 1, so the similar samples can be used in the experiment to simulate coal samples of high strength.

4.4. Experimental Process. Based on the experience with using HVEP for enhancing the production of oil, it is feasible to use the electrode to crush samples in water condition. In brief, the experimental process involves the following steps: (1) Before the experiments, the distance between the electrodes is adjusted, the electrode is then placed in the water environment, the electrical capacitor is charged, and then the switch is opened to test the reliability of the HVEP system. (2) For similar samples, some water is injected into the borehole, and the height of the water is half of the length of the hole; then the electrode is placed in the hole and the borehole is pressed to simulate the sealing situation. For coal samples, a box is

made to place the coal samples to avoid shaking in the process of the electrohydraulic crushing, the electrode is placed into the box that is full of water, then the coal samples are placed under the electrode. (3) The electrical capacitors are charged until the level of the capacitors meets the electrical field strength, then the trigger switch is turned on, and the electrode will discharge to break the samples. (4) The above steps are repeated until the samples are broken down.

The distance between the anode and cathode can be adjusted in the experimental process. Assuming the electric field strength between the anode and the cathode of the electrodes is E,

$$E = \frac{U}{d} \tag{5}$$

where U is the voltage between the anode and cathode, and d is the distance between them.

Assuming the max pressure of shock wave when the electrode is discharged in water condition is p_m,

$$p_m = \beta \sqrt{\frac{\rho_0 W}{\tau T}} \tag{6}$$

where β is the complex integral function without dimension, ρ_0 is the density of the liquid, W is the discharge energy of the electrode, T is the pulse duration time, and τ is the wave front time.

The breakdown field strength under different voltages in water environment is calculated using eqs 5 and 6. The electric field strength can be changed by the distance of the electrodes and the discharge voltage. In the experiments, the samples would be cracked after being crushed many times.

■ AUTHOR INFORMATION

Corresponding Authors

Hongqi Lu − *School of Management Engineering, Zhengzhou University of Aeronautics, Zhengzhou 450046, China; College of Safety Science and Engineering, Henan Polytechnic University, Jiaozuo 454003 Henan, China;* ● orcid.org/0000-0002-4255-1906; Email: cumtblhq@163.com

Baisheng Nie − *School of Resources and Safety Engineering, Chongqing University, Chongqing 400044, China;*

○ orcid.org/0000-0003-3575-5801; Email: bshnie@163.com

Authors

Yanwei Liu − *College of Safety Science and Engineering, Henan Polytechnic University, Jiaozuo 454003 Henan, China*

Xiujuan Chen − *State-owned Assets Management Department, Zhengzhou University of Aeronautics, Zhengzhou 450046, China*

Xiaokai Xu − *School of Energy Science and Engineering, Henan Polytechnic University, Jiaozuo 454003 Henan, China*

Complete contact information is available at:
https://pubs.acs.org/10.1021/acsomega.1c04515

Notes

The authors declare no competing financial interest.

■ REFERENCES

(1) Mu, F. Y.; Zhong, W. Z.; Zhao, X. L.; Che, C. B.; Chen, Y. P.; Zhu, J.; Wang, B. Strategies for the development of CBM gas industry in China. *Nat. Gas Ind. B* **2015**, *2*, 383−389.

(2) Yutkin, L. A. *Electro-Hydraulic Effect*; US Department of Commerce, Office of Technical Service, 1955.

(3) Sarkis, J. R.; Nadia, B.; Isabel, C.; Ligia, D. F. M.; Eugène, V. Application of pulsed electric fields and high voltage electrical discharges for oil extraction from sesame seeds. *J. Food Eng.* **2015**, *153*, 20−27.

(4) Andres, U.; Jirestig, J.; Timoshkin, I. Liberation of minerals by high-voltage electrical pulses. *Powder Technol.* **1999**, *104*, 37−49.

(5) Zuo, W. R.; Shi, F. N.; Klaas, P. W.; Weh, A. Ore particle breakage behaviour in a pilot scale high voltage pulse machine. *Miner. Eng.* **2015**, *84*, 64−73.

(6) Sperner, B.; Jonckheere, R.; PfäNder, J. A. Testing the influence of high-voltage mineral liberation on grain size, shape and yield, and on fission track and 40Ar/39Ar dating. *Chem. Geol.* **2014**, *371*, 83−95.

(7) Lu, X. P.; Zhang, H. H.; Pan, X.; Liu, K. F.; Liu, M. H. Study on the pressure characteristics of pulsed discharge in water. *Explosion Shock Waves* **2001**, *21*, 282−286.

(8) Kai, Z.; Feilong, S.; Di, J.; et al. Experimental investigation on the cracking of pre-combustion cracking gas with gliding arc discharge plasma. *Int. J. Hydrogen Energy* **2021**, *46*, 9019−9029.

(9) Andres, U.; Timoshkin, I.; Jirestig, J.; Stallknecht, H. Liberation of valuable inclusions in ores and slags by electrical pulses. *Powder Technol.* **2001**, *114*, 40−50.

(10) Andres, U. Dielectric separation of minerals. *J. Electrostat.* **1996**, *37*, 227−248.

(11) Sperner, B.; Raymond, J.; Jörg, A. P. Testing the influence of high-voltage mineral liberation on grain size, shape and yield, and on fission track and 40Ar/39Ar dating. *Chem. Geol.* **2014**, *371*, 83−95.

(12) Tao, R.; Xu, X. Reducing the Viscosity of Crude Oil by Pulsed Electric or Magnetic Field. *Energy Fuels* **2006**, *20*, 2046−2051.

(13) Zuo, W. R.; Shi, F. N. Ore impact breakage characterisation using mixed particles in wide size range. *Miner. Eng.* **2016**, *86*, 96−103.

(14) Bru, K.; Solène, T.; Pascal, A.; et al. Investigation of lab and pilot scale electric-pulse fragmentation systems for the recycling of ultra-high performance fibre-reinforced concrete. *Miner. Eng.* **2018**, *128*, 187−194.

(15) Duan, C. L.; Diao, Z. J.; Zhao, Y. M.; Huang, W. Liberation of valuable materials in waste printed circuit boards by high-voltage electrical pulses. *Miner. Eng.* **2015**, *70*, 170−177.

(16) Patel, K.; Manan, S.; Anirbid, S. Plasma Pulse Technology: An uprising EOR technique. *Pet. Res.* **2018**, *3*, 180−188.

(17) Bai, L. L.; Zheng, L.; Wang, Y.; Yan, T.; Sun, W. F.; Li, Z. X.; Liu, S. C. Study on the law of the effect of rock pore properties on the electric pulse rock breaking. *SPE Oil Gas Reservoir* **2021**, *28*, 148−153.

(18) He, J. Y.; Zhang, R. S.; Zhang, J. C.; Liu, M. J.; Izuchukwu, O. N. Experimental evaluation of near wellbore stimulation-using electrical explosion shockwave on tight sand reservoir. *Oil Gas Sci. Technol.* **2018**, *73*, 60−69.

(19) Chen, W.; Maurel, O.; Reess, T.; Ferron, A. S. D.; Borderie, C. L.; Gilles, P. C.; Franck, R. B.; Jacques, A. Experimental study on an alternative oil stimulation technique for tight gas reservoirs based on dynamic shock waves generated by pulsed arc electrohydraulic discharges. *J. Pet. Sci. Eng.* **2012**, *88−89*, 67−74.

(20) Yan, F. Z.; Lin, B. Q.; Zhu, C. J.; Guo, C.; Zhou, Y.; Zou, Q. L.; Liu, T. Using high-voltage electrical pulses to crush coal in an air environment: An experimental study. *Powder Technol.* **2016**, *298*, 50−56.

(21) Yan, F. Z.; Lin, B. Q.; Zhu, C. J.; Zhou, Y.; Liu, X.; Guo, C.; et al. Experimental investigation on anthracite coal fragmentation by high-voltage electrical pulses in the air condition: Effect of breakdown voltage. *Fuel* **2016**, *183*, 583−592.

(22) Zhang, X. L.; Lin, B. Q.; Shen, J. Experimental research on the effect of plasma on the pore-fracture structures and adsorption-desorption of coal body. *Fuel* **2022**, *307*, No. 121809.

(23) Li, H. L.; Qin, Y.; Zhang, Y. M.; Shi, Q. M.; Zhou, X. T. Experimental study on the effect of strong repetitive pulse shockwave on pore structure of fat coal. *J. China Coal Soc.* **2015**, *40*, 915−921.

(24) Qin, Y.; Li, H. L.; Zhang, Y. M.; Zhao, Y. Z.; Zhao, J. C.; Qiu, A. C. Numerical nanlysis on CSW fracturing behavior of coal seam under constraint of geological and engineering conditions. *Coal Geol. Explor.* **2021**, *49*, 108−119.

(25) Ma, S. Q. Research on coal seam permeability improvement by high-voltage electric pulse discharge. *Saf. Coal Mines* **2019**, *50*, 15−18.

(26) Zhang, Y. M.; Meng, Z. Z.; Qin, Y.; Zhang, Z. F.; Zhao, Y. Z.; Qiu, A. C. Innovative engineering practice of soft coal seam permeability enhancement by controllable shock wave for mine gas extraction: A case of Zhongjing Mine, Shuicheng, Guizhou Province, China. *J. China Coal Soc.* **2019**, *44*, 2388−2400.

(27) Zhang, Y. M.; An, S. G.; Chen, D. F.; Shi, Q. M.; Zhang, Z. H.; Zhao, Y. Z.; Luo, H. G.; Qiu, A. C. Preliminary Tests of Coal Reservoir Permeability Enhancement by Controllable Shock Waves in Baode Coal Mine 8# Coal Seam. *Saf. Coal Mines* **2019**, *50*, 14−18.

(28) Wu, J.; Tian, Y. D. Application of high energy electric pulse technology in coalbed methane wells in Qinshui basin. *Coal Geol. Explor.* **2018**, *46*, 206−212.

(29) Guo, Z. D.; Zeng, W. T.; Fang, H. J.; Ge, T. Z.; Han, J.; Lin, J. D. Initial application of intense repeated pulse wave for stimulation CBM reservoirs. *China Pet. Explor.* **2019**, *24*, 397−402.

(30) Zhang, C.; Li, M. X.; Wang, L. L.; Shi, H. Y.; Wang, J. EOR measures for CBM gas wells and their practices in Fanzhuang block, southern Qinshui basin. *Nat. Gas Ind.* **2011**, *31*, 116−120.

(31) Ma, Z. Z.; Zhao, J. C.; Zhao, Y. X.; Qin, S. Study on the law of coal and rock mass fracturing with different strength by pulse discharge stress wave. *China Miner. Mag.* **2021**, *30*, 135−140.

(32) Chu, H. B.; Yang, X. L.; Yu, Y. Q. Experimental research of the choice for coal blasting simulation material. *Coal Sci. Technol.* **2010**, *38*, 31−33.

(33) Chu, H. B. Theoretical and Experimental Studies On Coal Blasting Action Mechanism, Doctoral Dissertation, Henan Polytechnic University: Jiaozuo, 2011.

(34) Fu, R. Y.; Sun, Y. H.; Fan, A. L.; Gao, Y. H.; Yan, P.; Zhou, J. Research of rock fracturing based on high voltage pulse in shale gas drilling. *High Power Laser Part. Beams* **2016**, *28*, 1−5.

(35) Stöbener, D.; Gabriela, A.; Lasse, L.; Marius, H.; Christian, S.; Andreas, F. An optical method to determine the strain field on micro samples during electrohydraulic forming. *Proc. CIRP* **2020**, *87*, 438−443.

(36) Krooss, B. M.; Van, B. F.; Gensterblum, Y.; Siemons, N.; Pagnier, H. J. M.; David, P. High-pressure methane and carbon dioxide adsorption on dry and moisture equilibrated Pennsylvanian coals. *Int. J. Coal Geol.* **2002**, *51*, 69−92.

(37) Masoudian, M. S.; David, W. A.; Abbas, E. Experimental investigations on the effect of CO_2 on mechanics of coal. *Int. J. Coal Geol.* **2014**, *128*, 12−23.

(38) Lu, X. P.; Pan, Y.; Zhang, H. H. A study on the characteristic of plasma and bubble break process of pulsed discharge in water. *Acta Phys. Sin.* **2002**, *51*, 1768−1772.

(39) Rajoriya, S.; Jitendra, C.; Virendra, K. S.; Aniruddha, B. P. Hydrodynamic cavitation: an advanced oxidation process for the degradation of bio-refractory pollutants. *Rev. Chem. Eng.* **2016**, *32*, 379−411.

(40) Yang, J. F.; Lian, H. J.; Liang, W. G.; et al. Experimental investigation of the effects of supercritical carbon dioxide on fracture toughness of bituminous coals. *Int. J. Rock Mech. Min. Sci.* **2018**, *107*, 233−242.

(41) *CBM Development and Utilization of the "13th Five-Year" Plan*; National Energy Administration: Beijing, 2016.

(42) Suchy, D. R.; Newell, K. D. *Hydraulic Fracturing of Oil and Gas Wells in Kansas*, Kansas Geological Survey, Public Information Circular, 2011.

(43) Yan, Q. B.; Ma, L. C.; Huang, X. A technology of compound fracturing. *Fault Block Oil Gas* **2004**, *11*, 74−76.

(44) Qu, D. *Research on the DM-2 Electric Pulse Equipment*; China University of Geosciences: Beijing, 2002.